Instrument Science Report STIS 2015-04

Photometric Performance of STIS CCD CTI Corrections on Omega Cen Images

John Biretta, Sean Lockwood, and John Debes

September 28, 2015

ABSTRACT

We compare the photometric performance of empirical and pixel-based Charge Transfer Inefficiency (CTI) corrections for the STIS CCD detector using imaging observations of the star cluster Omega Cen. Two tests are performed: The first examines the long-term photometric trend using 22 datasets spanning the STIS mission, while the second test examines the Y-dependence of CTI by comparing amp A and amp D data at a single epoch in 2012. These two tests draw on relatively independent data sets, and have only the single 2012 amp D dataset in common. The two tests give similar results. The empirical and pixel-based corrections both significantly improve the photometric accuracy across a wide range of stellar magnitudes. For the brightest stars (mag<18) the CTI effect itself is small, and differences between the two correction methods are small (<0.02 mag). Between mag=18 and 19 the empirical corrections appear more accurate, but the error for the pixel-based correction is only 0.02 mag near the detector center. At fainter magnitudes (mag=19 to 22) where CTI is larger, the empirical corrections ***over****-correct the photometry by 26% to 42%, while the pixel-based corrections* ***under****-correct by 29% to 34% of the total CTI effect. There is some evidence that the pixel-based corrections are more stable between different magnitude ranges, and may lead to better relative photometry. We describe additional tests that could be performed in the future.*

Operated by the Association of Universities for Research in Astronomy, Inc., for the National Aeronautics and Space Administration

1. Introduction

Empirical Charge Transfer In-efficiency (CTI) corrections have been available for the STIS CCD photometry for many years (Goudfrooij 2006). These corrections compare the observed magnitudes of stars with their true magnitudes, and provide a correction which is a function of location on the detector, observed stellar counts, image background counts, and observation epoch. Efforts are now underway to implement *pixel-based* CTI corrections for the STIS CCD detector (Anderson and Bedin, 2010; Lockwood, et al. 2013, 2014a). These pixel-based corrections attempt to model the detector-level physics of CTI effects, and then correct each pixel of the image to the proper counts with CTI effects removed. Pixel-based corrections have several potential advantages: besides correcting the photometry, they can remove trails on cosmic ray hits and hot pixels, thereby reducing artifacts and the background noise in images. Pixel-based corrections can also correct photometry and target structure for complex scenes which are beyond the scope of simple empirical corrections derived from stellar images.

The pixel-based correction algorithm we employ is based on the work of Anderson and Bedin (2010) for the ACS WFC detector. The algorithm works by iteratively relocating counts on the detector to nearby pixels, based on a model of the expected CTI effects. The same computer code is used here for STIS, though with new model parameters derived for the STIS CCD detector (Lockwood 2012, 2013). Model parameters for STIS have been derived using hot pixels in dark frames, where single-pixel sources in the detector become smeared-out and trailed as a result of CTI effects. The model parameters are adjusted until the hot pixels are restored to being single-pixel events on the detector (Lockwood 2014a, 2014b; Lockwood, et al., 2015).

Herein we test the relative accuracy of the empirical and pixel-based CTI corrections for stellar photometry. Two separate tests are performed – the first examines long-term trends in the photometry, and the second compares data read out through amplifiers on opposite sides of the CCD (amp A vs. amp D) late in the STIS mission. Section 3 details the results of the two tests, while Section 4 summarizes and synthesizes the results. Section 5 makes recommendations for additional future tests. The Appendix presents detailed plots for the second test.

2. Data

In this section we describe the images used, the imaging processing, and the photometric measurements.

2.1. Data Selection

Table 1 lists the Omega Cen images used herein. All the images utilize the CLEAR filter, the 50CCD aperture, the MIRVIS grating, and are taken at CCDGAIN=4. The majority of the images are taken with CCDAMP=D (the default amplifier), though one is taken with CCDAMP=A and is used for a special test described later on. Each exposure consists of either two or three sub-frames with the individual exposure time listed as MEANEXP, and total exposure time listed as TEXPTIME. The entry PA_APER gives the position angle of the aperture on the sky.

Table 1. Omega Cen images used herein.

Image Name	Prop ID	DATE-OBS	MEANEXP (sec)	TEXPTIME (sec)	PA_APER (deg)	CCDAMP
o3zf01010_sx2.fits	7079	5/24/1997	20	60	7.66	D
o3zf01020_sx2.fits	7079	5/24/1997	20	60	7.66	D
o3zf01030_sx2.fits	7079	5/24/1997	20	60	7.66	D
o3zf01040_sx2.fits	7079	5/24/1997	20	60	7.66	D
o3zf01090_sx2.fits	7079	5/24/1997	21.33	64	7.66	D
o3zf010b0_sx2.fits	7079	5/24/1997	24	72	7.66	D
o3zf010c0_sx2.fits	7079	5/24/1997	24	72	7.66	D
o3zf010d0_sx2.fits	7079	5/24/1997	24	72	7.66	D
o3zf010e0_sx2.fits	7079	5/24/1997	24	72	7.66	D
o3zf010f0_sx2.fits	7079	5/24/1997	24	72	7.66	D
o3zf010g0_sx2.fits	7079	5/24/1997	24	72	7.66	D
o69902020_sx2.fits	8847	2/03/2001	30	60	-94.98	D
o6ib01020_sx2.fits	8912	9/01/2001	30	60	89.84	D
o6ib02020_sx2.fits	8912	2/15/2002	30	60	-94.98	D
o8h701050_sx2.fits	9622	2/05/2003	30	60	-94.98	D
o8uv01050_sx2.fits	10028	3/20/2004	30	60	-72.90	D
obat01050_sx2.fits	11854	1/30/2010	30	60	-94.98	D
obmj01050_sx2.fits	12409	2/05/2011	30	60	-94.98	D
obuo01050_sx2.fits	12770	2/10/2012	30	60	-94.98	D
obuo01090_sx2.fits	12770	2/10/2012	30	60	-94.98	A
oc5401050_sx2.fits	13139	1/31/2013	30	60	-94.98	D
ocfg01050_sx2.fits	13542	2/15/2014	30	60	-94.98	D
ocrj01050_sx2.fits	13989	2/04/2015	30	60	-94.98	D

We elected to use only a subset of the images used by Roman-Duval and Proffitt 2013 (hereinafter RP2013; their Table 4), so as to maximize uniformity of the data. Exposures with individual exposure times (MEANEXP) less than 20 seconds were avoided, so as to maximize the signal-to-noise ratio. Only gain 4 images were used, so as to avoid saturation effects. And the 2000 data from proposal 8047 were omitted as the target acquisition failed and the shutter did not open. We also added new images taken since RP2013 from proposals 13139, 13542, and 13989.

2.2. Image Calibration and Processing

Farther below we will study three cases of CTI correction: no correction, empirical correction, and pixel-based correction. The standard archive *_sx2.fits products were used for the uncorrected and empirically corrected cases. For the pixel-based corrected case, the data were manually processed as follows. First the normal BIASLEV, BIASCORR, and DQICORR calibrations were applied using the BASIC2D task in the STIS STSDAS package.

Pixel-based CTI corrections were then applied using the StisPixCteCorr python task, along with the reference file TEST_PCTE.FITS (Anderson and Bedin 2010, Lockwood, et al., 2013, 2014a, 2014b, 2015). Our user-settable parameters in the CTE reference file header are listed in Table 2. These are, in order, SIM_NIT which is number of readout simulation iterations performed on each image column, SHFT_NIT which is the number of shift iterations on each column, RN_CLIP which is an estimate of the image read noise in electrons, NSEMODEL which selects the noise model and can be used to limit CTI corrections at very low signal levels based on RN_CLIP, and SUBTHRSH which is the over-subtraction correction threshold which limits the maximum difference (corrected image - original image). We found that adjustments to the first two parameters had very little effect. Our choice of NSEMODEL=0 and SUBTRESH=-200 causes pixels of all brightness to be corrected.[1]

Table 2. TEST_PCTE.FITS parameters.

Parameter	Value
SIM_NIT	7
SHFT_NIT	4
RN_CLIP	5.6
NSEMODEL	0
SUBTHRSH	-200

[1] NSEMODEL=0 turns-off the lower brightness limit for the corrections, and disables use of the RN_CLIP parameter. SUBTHRSH is the lowest allowed value for the difference (corrected image – original image) and can limit correction of very bright pixels. The value -200 effectively removes this limitation, and allows very bright pixels to receive the full correction.

Finally the remaining standard calibrations (DARKCORR, FLATCORR, etc.) were applied using CALSTIS. In all cases the normal pipeline / archive reference files were used.[2]

2.3. Photometric Measurements

Our photometric procedures closely followed those of RP2013, and the reader is referred there for most details. We used the same IDL scripts wherever possible. Some slight differences would arise where, for example, we used the current IDL version of the IDL APER procedure, whereas RP2013 necessarily used an older version.

Initially we used the same catalog of 123 stars from Figure 2 in RP2013 which was derived from image obat01050_sx2.fits, which served as the reference image. The catalog was then edited in a number of ways. We blinked this image against the data from later epochs and identified several stars which appeared fixed in detector coordinates, and these were eliminated as being hot pixels. We also eliminated several stars from the catalog where bright hot pixels were present in the 33x33 pixel sub-image[3] in either the reference image or a large number of other images. Several new stars were also added to our catalog, so as to keep the total number of stars above 100. The final catalog of 119 stars is shown in Figure 1.

The images taken after 1997 were generally well-aligned with the reference image, and nearly the full catalog of stars was available for each image. However, the 1997 data had a significantly different pointing, and only about one-quarter of the catalog stars were available. A typical scenario for the 1997 data is shown in Figure 2. These data also had small position dithers so more or less numbers of stars might be available than this example.

Star images were checked for saturation effects. The brightest star contained ~36,000 DN in the central pixel of the PSF, and so slightly exceeds the 130,000 e- full-well, but is still well within the limits where accurate photometry can be performed (e.g. Gilliland, Goudfrooij & Kimble, 1999).

Finally the data were further edited by discarding stars within a 100 pixel border around the edges of the image. This border excludes regions where the star aperture or sky annulus might be impacted by the 50CCD aperture mask. It also serves to exclude the 38 pixel empty

[2] We did not apply pixel-based CTI corrections to the dark reference files. We ran a test using CTI-corrected darks for one image, and found it did not significant alter the photometry or astrometry. For long exposures this would reduce artifacts and improve the signal-to-noise ratio, but for our short exposures there was no significant impact on the results.

[3] That is, the 33x33 pixel sub-image used for photometric measurement.

border of the 1100x1100 pixel *_sx2.fits files.

Aperture photometry was performed with the IDL APER procedure using an aperture radius of 5 times the FWHM of the PSF. The sky annulus had the same inner radius, and a thickness of 5 pixels. The nominal PSF FWHM was about 1.8 pixels, leading to an aperture radius of about 4.5 pixels. Net counts were converted to magnitudes using Equation 1 of RP2013, which includes corrections for long-term changes in the instrument and telescope sensitivity via their ZMAG parameter. Our equation (1) below defines ZMAG in terms of the PHOTFLAM and PHOTZPT image header keywords. ZMAG is plotted vs. time for our observations in Figure 3.

$$ZMAG = -2.5 \log_{10}(PHOTFLAM) + PHOTZPT \qquad (1)$$

We compared our photometric results to those of RP2013 for data common to the two datasets. For the brighter stars the results agreed to better than 0.01 mag, while differences of 0.02 mag were seen for the fainter stars. In all cases the differences were much smaller than the photometric uncertainties.

When testing the empirical CTI corrections, we calculated the corrections from the equations in Goudfrooij, et al., 2006. These corrections depend on the average star counts (in e-) in the individual sub-frames or IMSETs of the observation, the average counts per pixel in the sky annulus (in e-/pixel), the Y position of the star on the detector, and the observation date. These corrections were applied to the aperture photometry results. We did not use the STSDAS CTESTIS routine for the corrections as RP2013 had done, but rather coded these into a new IDL routine. The purpose of the new routine was to speed-up the calculations. The new IDL routine was extensively tested against both the STSDAS version and the equations in Goudfrooij, et al., 2006, and found to have excellent agreement for the photometry corrections used herein.

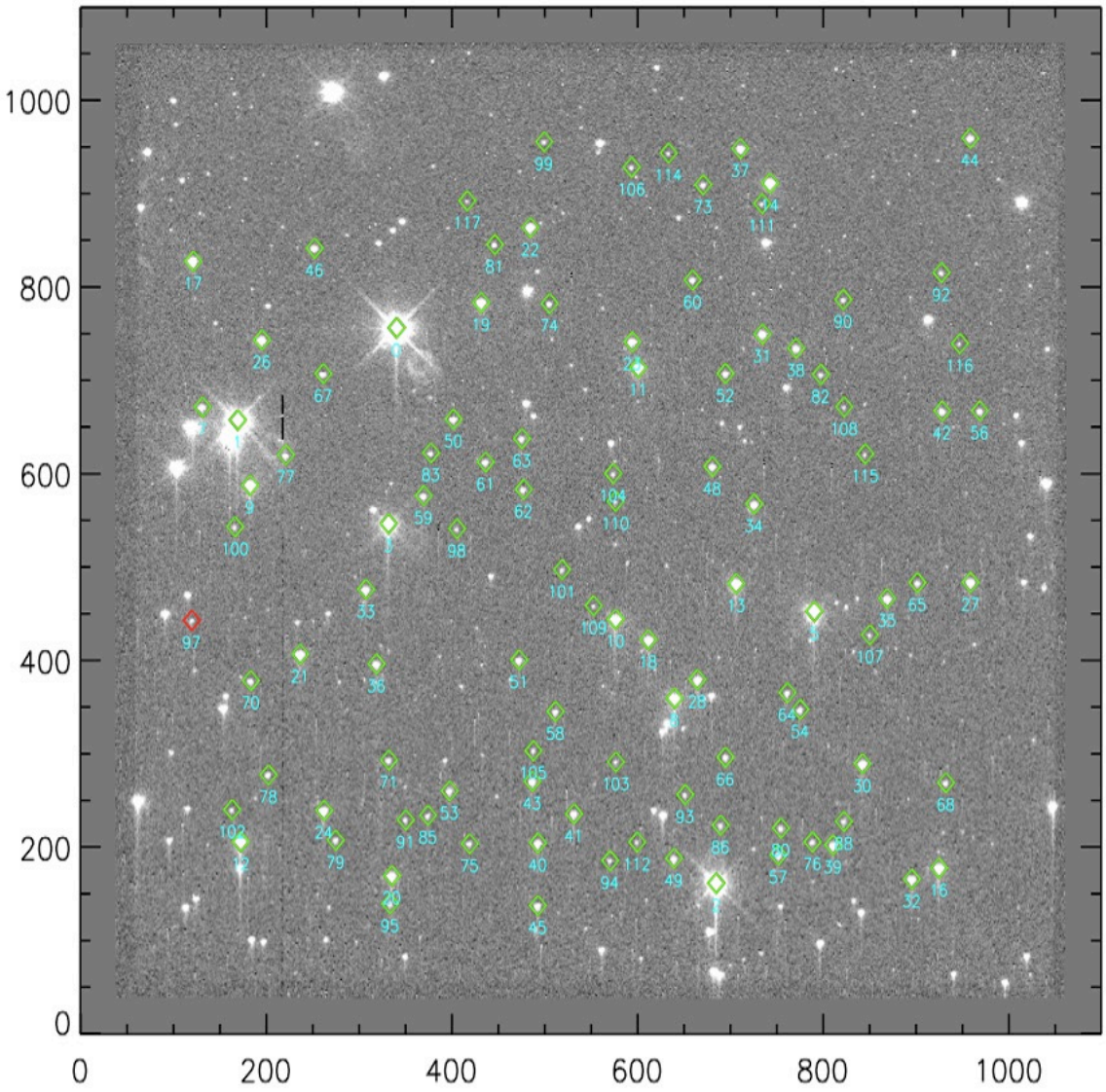

Figure 1. Reference image obat01050_sx2.fits with the catalog of 119 stars indicated. Pixel coordinates are indicated along the X and Y axes. The geometrically corrected *_sx2.fits format images include a 38 pixel buffer on all sides, and hence are 1100 x 1100 pixels. Star 97 (marked in red) had discrepant photometry and was excluded for this particular image.

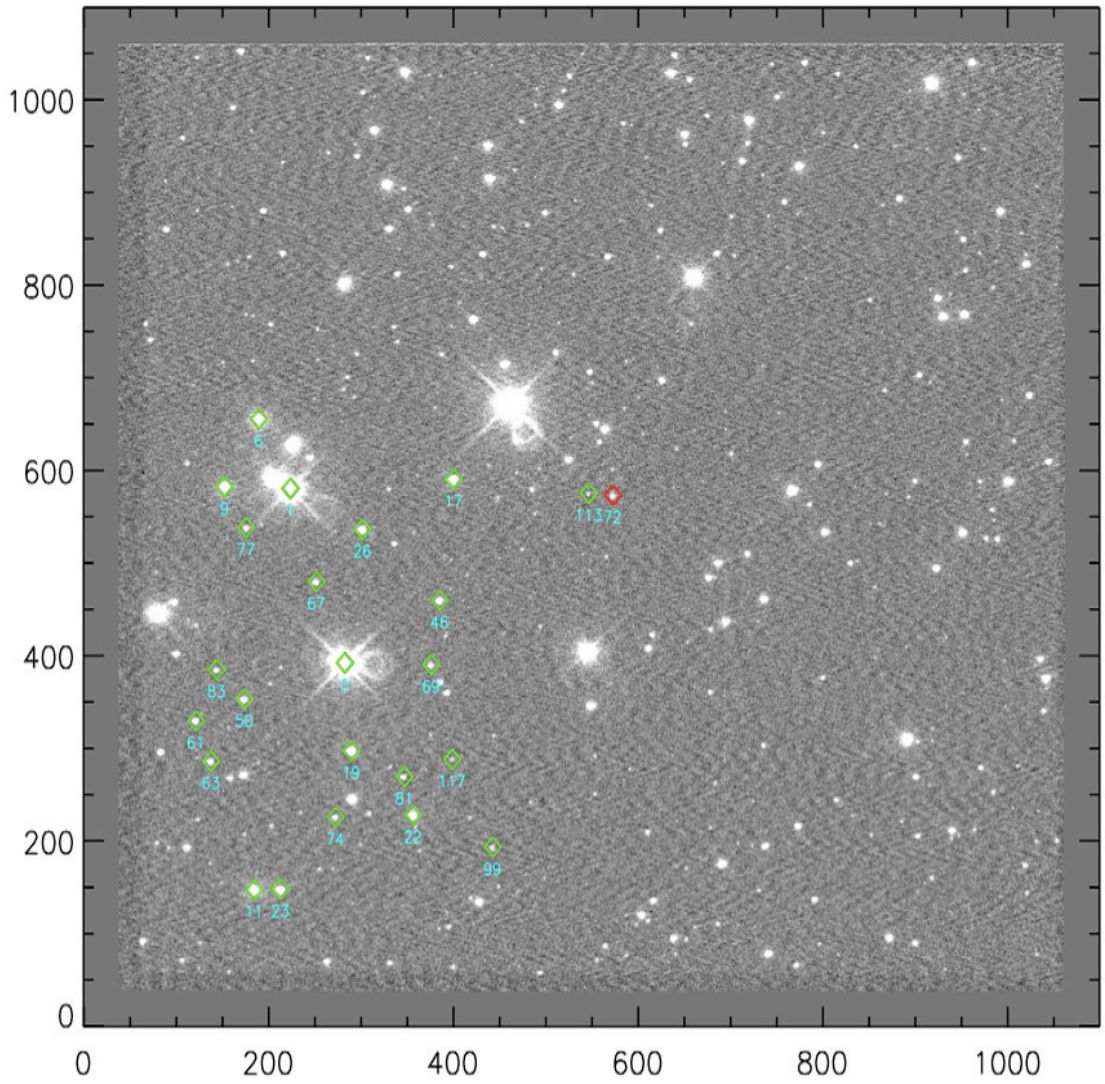

Figure 2. Image o3zf01010_sx2.fits with catalog stars indentified. Pixel coordinates are indicated along the X and Y axes. Star 72 (marked in red) had discrepant photometry and was excluded for this particular image.

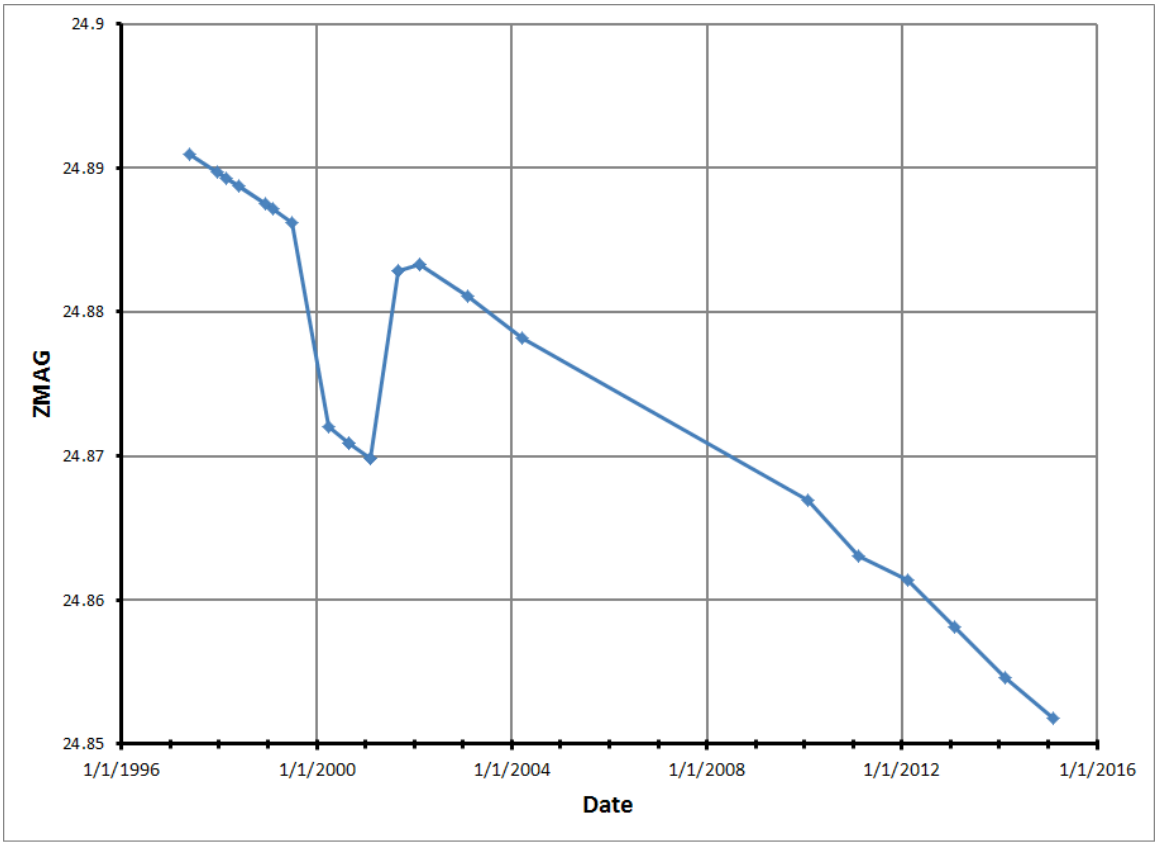

Figure 3. Plot of ZMAG photometric calibration vs. date for our datasets. ZMAG is computed using equation 1 and the values of PHOTFLAM and PHOTZPT in the header of each image.

3. Analyses and Results

The photometric information collected above was then used to perform two different tests on the photometric CTI corrections. In the first test, we examine long-term trends in the photometric calibration due to CTI effects. In the second test, we examine the Y-dependence of the photometry using data read out through the CCD "A" amplifier in addition to the default CCD "D" amplifier.

3.1. Long-Term Trends in the Photometric Calibration

Given the available data at this point, we can examine the long-term photometric behavior of each star in our catalog, and study the effects of no correction, the empirical CTI corrections, and the pixel-based CTI corrections. This type of test has several advantages and disadvantages. Among the advantages, is that it tests one of the

fundamental properties of CTI, which is that CTI should increase roughly linearly with time as the detector is exposed to radiation damage on-orbit. It is also capable of detecting changes in the photometry which might be independent of the CCD Y pixel coordinate – for example, any traps which might absorb charge from the image, and then release it on a time-scale which is long compared to the read out time. It also makes good use of the many epochs which are available, and utilizes a mode (CCDAMP=D) which is well-calibrated. We are comparing images of the same star with itself with similar exposure times, so there is little concern about photometric biases for bright vs. faint images, or calibration between different instruments.

The primary disadvantage of this test is that it is difficult to completely separate CTI effects from other long-term effects which impact the photometric stability of the STIS CCD camera. A separate set of time-dependent sensitivity (TDS) calibrations are routinely performed on the STIS CCD. The TDS calibration is primarily intended to adjust for the long-term build-up of permanent contaminants on the camera optics, and degradation or mirror coatings both in the HST OTA and the STIS instrument, etc. However, in practice, the TDS is calibrated by observing bright standard stars, the empirical CTI corrections are applied to the data, and then the PHOTFLAM values are adjusted to produce perfect long-term photometric stability (Bohlin and Goudfrooij 2003; Stys, Bohlin, and Goudfrooij 2004). Hence, we are likely to find that the empirical CTI corrections give perfect photometric stability for bright stars. Any errors or deficiencies in the empirical CTI corrections will have been compensated by opposite adjustments in the TDS (PHOTFLAM) calibration.[4]

On the other hand, as we will see later in section 3.2, the CTI loss for bright stars is only ~0.02 magnitude by the epoch 2012, or about 1 milli-mag/yr, which sets some bounds to the errors and uncertainties related to co-mingling of CTI and TDS effects. Moreover, the PHOTFLAM corrections themselves are only ~2 milli-mag/yr (Figure 3). Hence we can safely assume the uncertainties arising from TDS effects are about this same size, or 1 to 2 milli-mags/yr. An additional constraint is that TDS corrections are independent of magnitude, and can only affect the overall photometric scale. Any photometric trends exceeding a few milli-mag/yr, or which depend on magnitude, cannot be attributed to TDS effects. Also, TDS effects will not impact *relative* comparisons of photometry – e.g. comparison of uncorrected, empirical, and/or pixel-based CTI corrections would not be impacted. Later we will see that there are large variations in the photometry (>> a few milli-mag/yr) as a function of magnitude, and these can only arise from CTI effects.

[4] The TDS corrections enter our own photometry through application of the PHOTFLAM header keyword when we convert detected electrons to magnitudes.

An additional complication for this test, is that the telescope pointing used for the 1997 observations is different from that of the later observations. As can be seen by comparing Figure 1 and Figure 2, only about one-fourth of the catalog stars are observed in 1997.[5] On a positive note, the same telescope pointing was used for the 2001 to 2015 data, so nearly all the stars have a minimum of 14 years of data.

For this test we have used the "D" amplifier data listed in Table 1. Figure 4 shows STIS CCD images from early and late epochs in the STIS mission, respectively. The effects of CTI late in the mission are readily apparent – star images on the lower part of the detector (far from the CCD "D" amplifier) have become strongly trailed. Figure 5 compares the 2015 image without and with the pixel-based corrections. The CTI trails have been eliminated on all but the brightest stars and hot pixels.

Our analysis of long-term photometric trends begins by fitting straight lines to the magnitudes vs. time for each star. Separate fits are made for the data without CTI corrections, with empirical CTI corrections, and with pixel-based CTI corrections. Examples of the fits for a single star of middle-brightness are shown in Figure 6. When no CTI corrections are made, the star grows fainter at a rate of 5.7 milli-mag/yr, or about 0.10 magnitude total over the 18 year time-baseline. For this particular star, the empirical corrections tend to slightly over-correct producing photometry which brightens at a rate of -0.4 milli-mag/yr. The pixel-based corrections very slightly under-correct the photometry and produce a dimming of the star at a rate of 0.1 milli-mag/yr. We note the empirical and pixel-based corrections agree with each other for this star, when the fit uncertainties of ~1 milli-mag/yr are taken into account.

Next we plot the long-term photometric slope for all stars in the catalog. We have eliminated a number of stars where there was good data at only three or fewer epochs (e.g if the star was too near the image edge at many epochs). Results for the remaining 106 stars with no CTI correction applied are shown in Figure 7. As expected, the stars appear to become fainter with time, and the rate of brightness loss is greater at faint magnitudes. At the bright end (mag~16) counts are lost at a rate of ~2 milli-mag/yr, while at the faint end (mag~22) the rate is ~10 milli-mag/yr averaging over the many stars.

Results with empirical CTI corrections applied are shown in Figure 8. This plot is the equivalent to Figure 8 of RP2013, but with more data editing, and three years of additional data from 2013 to 2015. The empirical corrections work very well at bright magnitudes and give zero photometric slope. But this is expected, since the empirical corrections were used in computing the TDS corrections, which were in turn defined to

[5] The stars observed in 1997 are in the lower part of the detector far from the amplifier, and which will have higher CTI at later epochs. This could potentially introduce some biases in the results.

give zero photometric slope. At fainter magnitudes (mag>20) there is an increasing tendency for the empirical corrections to over-correct the photometry.

Pixel-based CTI correction results are shown in Figure 9. The pixel-based CTI corrections generally work well, and give results close to the empirical corrections. Throughout most of the magnitude range the pixel-based corrections under-correct by about +2 milli-mag/yr relative to the empirical corrections, which is equivalent to a total change of ~0.04 magnitudes over the 18 year life of the instrument. But this value is close to the uncertainties related to TDS effects, so we cannot say whether the empirical or pixel-based corrections are actually more correct here. At fainter magnitudes (mag>21) the pixel-based corrections appear to give good accuracy.

Figure 10 shows the results for all three CTI corrections together on a single plot, where the data have been averaged in 1-magnitude bins. The number of stars in each bin is indicated across the bottom of the plot. The error bars on this plot have been computed as follows: when only 1 or 2 stars are available, the uncertainty is taken as that on the measurements; when more stars are available, the uncertainty is computed as the RMS scatter on the data, divided by the square root of the number of stars. The overall vertical scale in this figure is uncertain by about 1-2 milli-mag/yr due to TDS effects previously discussed.

From Figure 10 we can see that the empirical and pixel-based CTI corrections both significantly improve the photometry as compared to un-corrected data. We make some detailed comparisons of the pixel-based and empirical corrections based on this figure:

1) At all magnitudes the pixel-based CTI corrections are smaller than the empirical CTI corrections. In general the pixel-based corrections lie about mid-way between no correction, and the larger empirical corrections.

2) The empirical CTI corrected data show about +1 milli-mag/yr photometric slope at the bright end, but then steadily drops-off to the point where it is over-correcting (negative slope) by about a few milli-mag/yr for stars with mag=20-22.

3) The pixel-based corrections produce a photometric slope between 0 and +2 milli-mag/yr across most of the magnitude bins. Due to the TDS effects this value is uncertain by about 1-2 milli-mag/yr, and so could be consistent with zero photometric slope.

4) At the faint end, for mag>21, both the empirical and pixel-based methods over-correct the CTI. The empirical method over-corrects by 9 milli-mag/yr, while pixel-based method over-corrects by 4 milli-mag/yr . These over-corrections are much larger than the 1-2 milli-mag/yr uncertainty contributed by TDS effects. At these magnitudes the pixel-based corrections appear more accurate than the empirical corrections.

5) The pixel-based corrections appear to give more uniform results across different magnitudes. For pixel-based corrections the photometric slopes range between and +2 and -4 milli-mag/yr (a range of 6 milli-mag/yr). On the other hand, the empirical corrections range between +1 and -9 milli-mag/yr (range of 10 milli-mag/yr). Hence the range in slopes is about half as large for the pixel-based corrections. The result is independent of the TDS effects.

6) The scatter between individual stars is often less for the pixel-based corrections. This can be seen by comparing Figure 8 and Figure 9 at middle magnitudes. And also by comparing the sizes of error bars in Figure 10.

Histograms of the photometric slopes are shown in Figure 11. The histogram for the empirical corrections is effectively equivalent to Figure 6 in RP2013. Both our work and RP2013 found that the histogram for the empirically corrected data peaked at slightly at slightly positive slopes near +1 milli-mag/yr. A broad tail of negative slope values (over-correction) is seen in our work.

We cannot attach much significance to the fact that the histogram peak for the empirically corrected data is closer to zero slope, than is that for the pixel-based corrected data. The TDS values have effectively been established to place the average photometric slope near zero, and that work assumed the empirical corrections as part of their analyses. The differences between the peaks of the histograms are roughly within the 1-2 milli-mag/yr uncertainty contributed by TDS effects.

The pixel-based corrections show a much higher peak in the histogram than the un-corrected or empirically corrected data, because many more stars have photometric slopes near +3 milli-mag/yr. This is partly because stars over a wide range in magnitudes have average slopes near this value, as mentioned above in connection with Figure 10 and items (3) and (5) above. And also because at a given magnitude the spread of slope values from one star to another tends to be smaller, as discussed in item (6) above. This result is not affected by uncertainties related to the TDS.

We note that some caution is needed in interpreting the histogram, since the uncertainties and scatter on the fainter stars cause them to appear as a broad base of the histogram. The peak of the histogram is dominated by brighter stars (mag < 20) with small scatter.

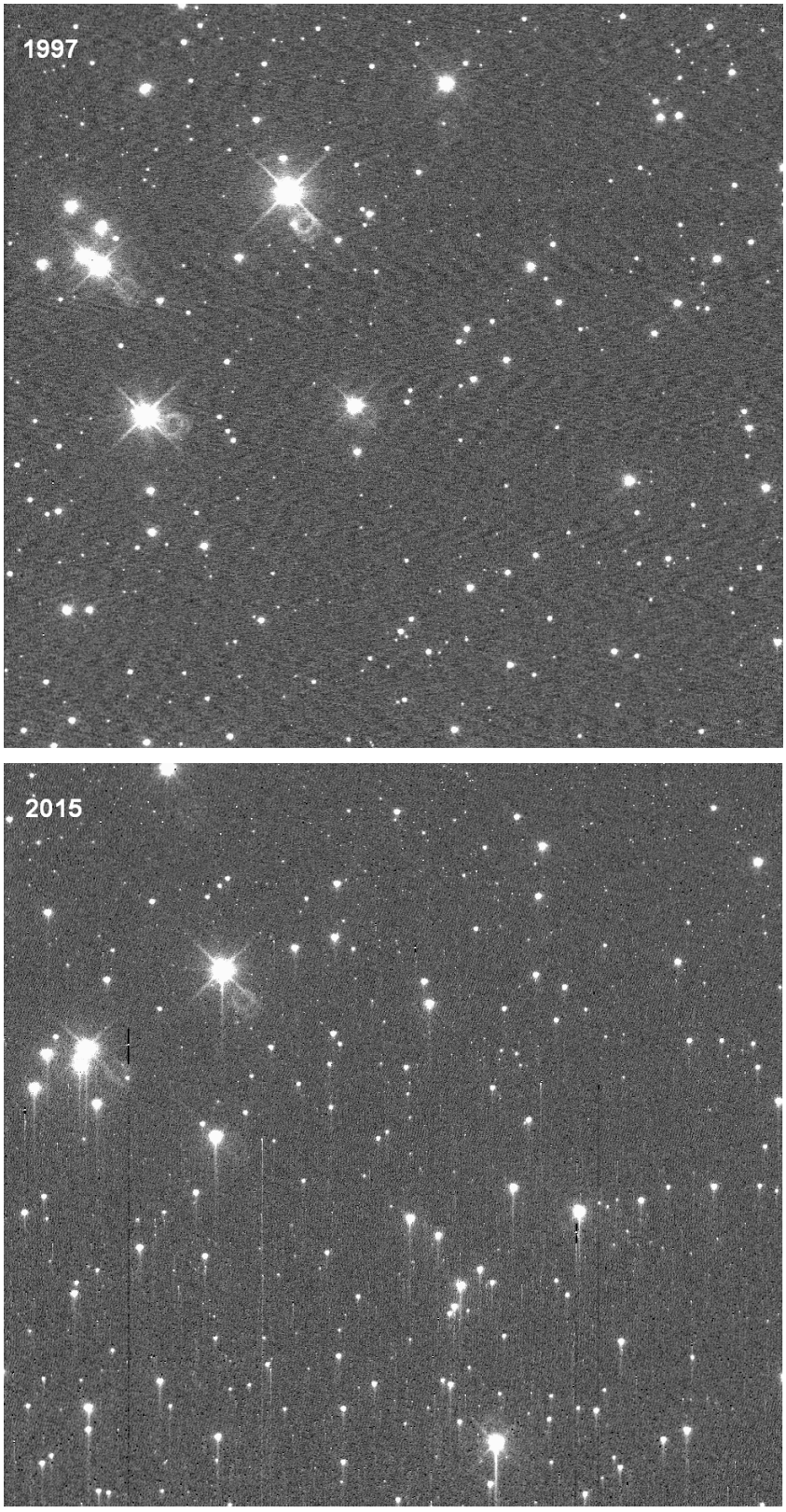

Figure 4. Comparison of uncorrected images from 1997 and 2015 illustrating the long-term increase in CTI. These are read-out using the D amplifier which is located at the top right corner of the images.

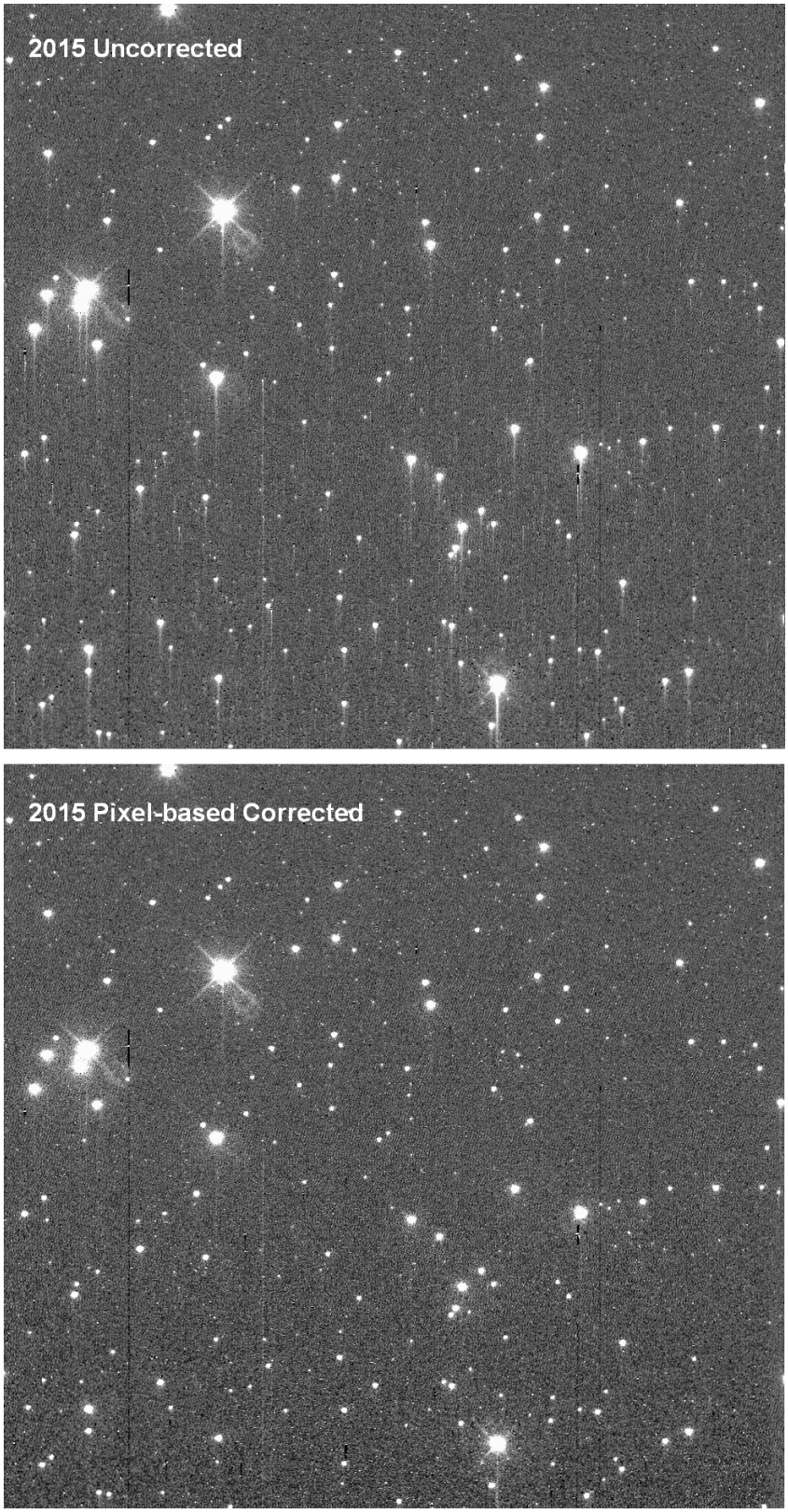

Figure 5. Comparison of 2015 uncorrected and pixel-based corrected images.

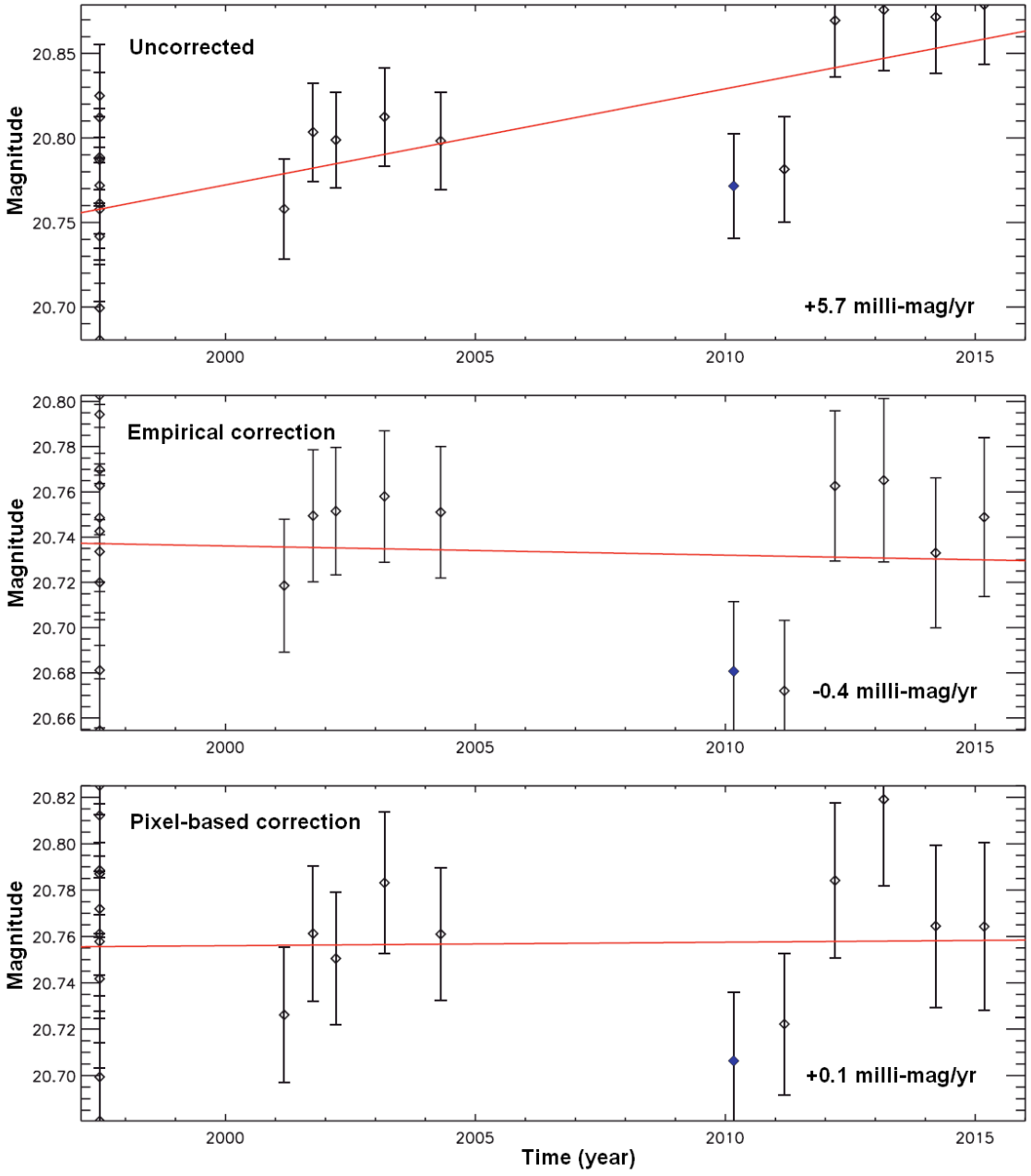

Figure 6. Sample magnitude vs. time fits for a representative star of middle brightness. Fitted slopes are indicated on each plot, and are uncertain by ~1 milli-mag/yr. The top panel shows photometry without any correction; the middle panel shows empirical corrections applied to the data in the top panel; and the bottom panel shows photometry on images where pixel-based corrections have been applied.

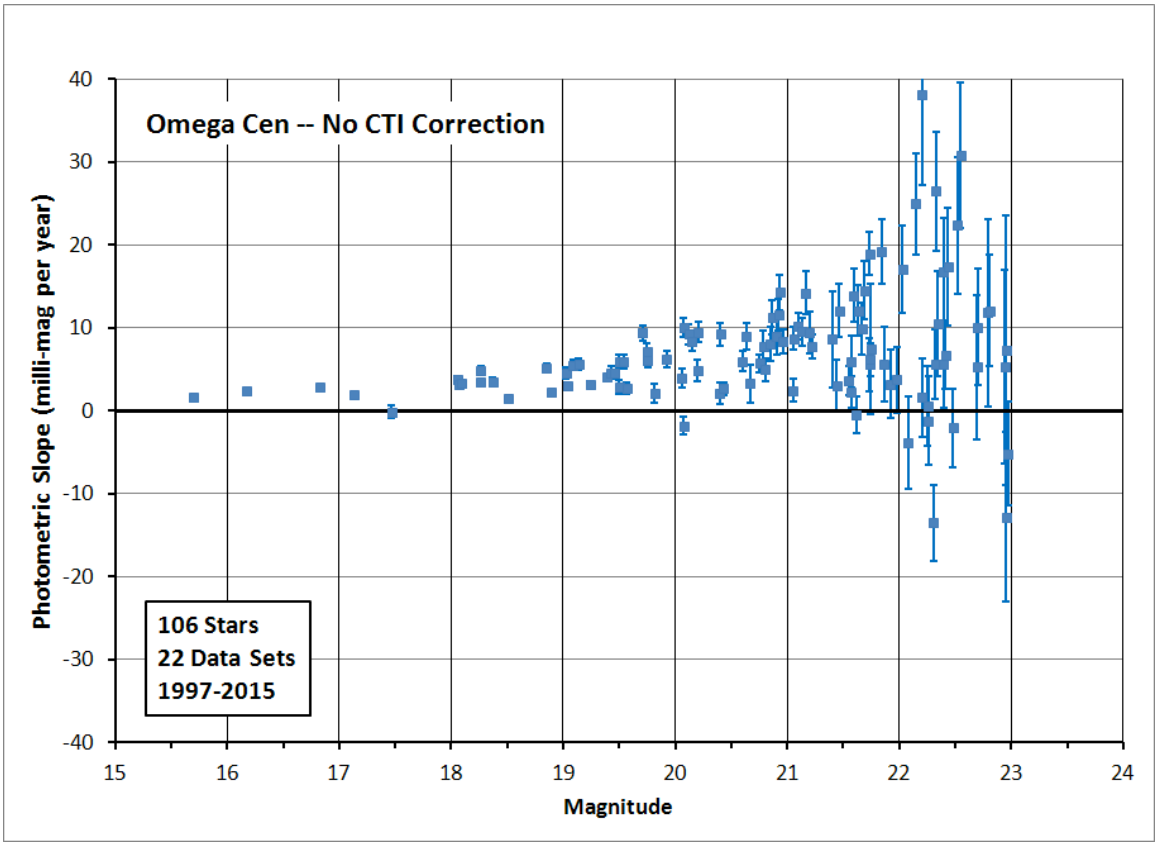

Figure 7. Long-term photometric slope plotted against magnitude for 106 stars with no CTI corrections.

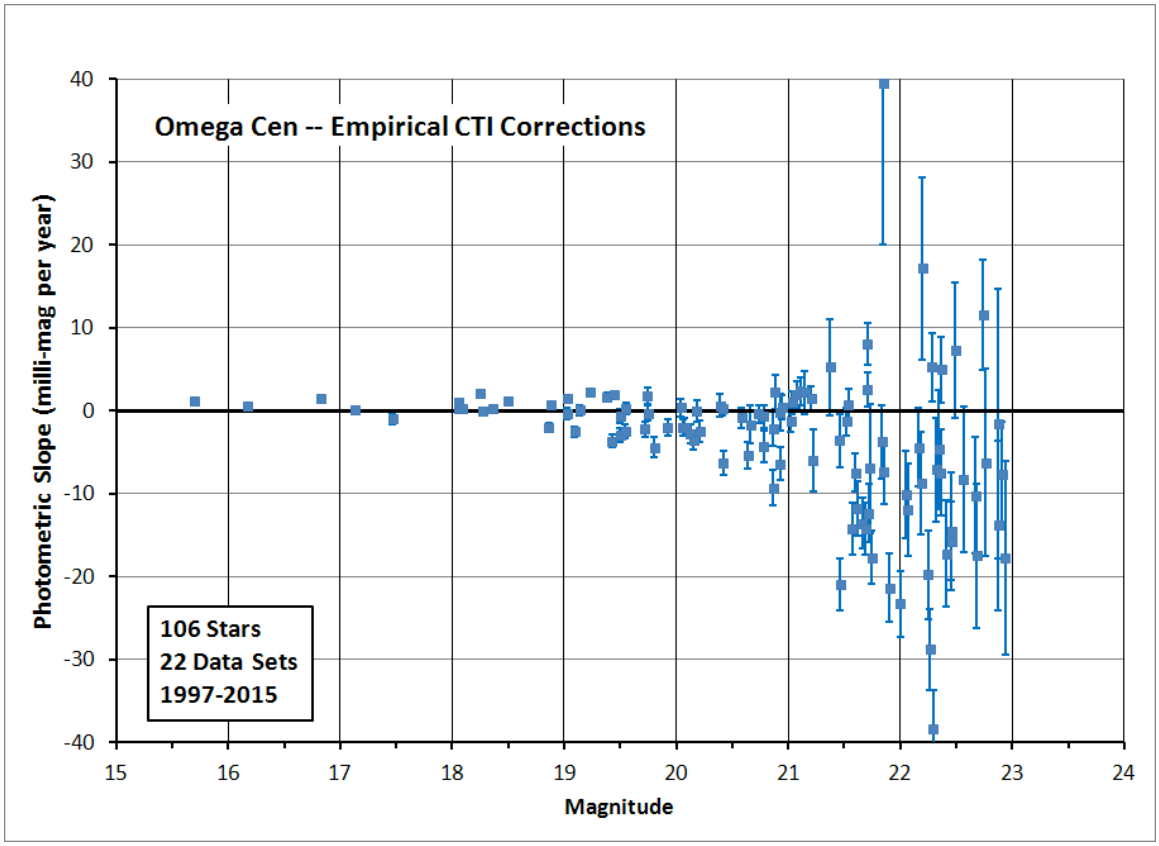

Figure 8. Long-term photometric slope plotted against magnitude for 106 stars with empirical CTI corrections applied.

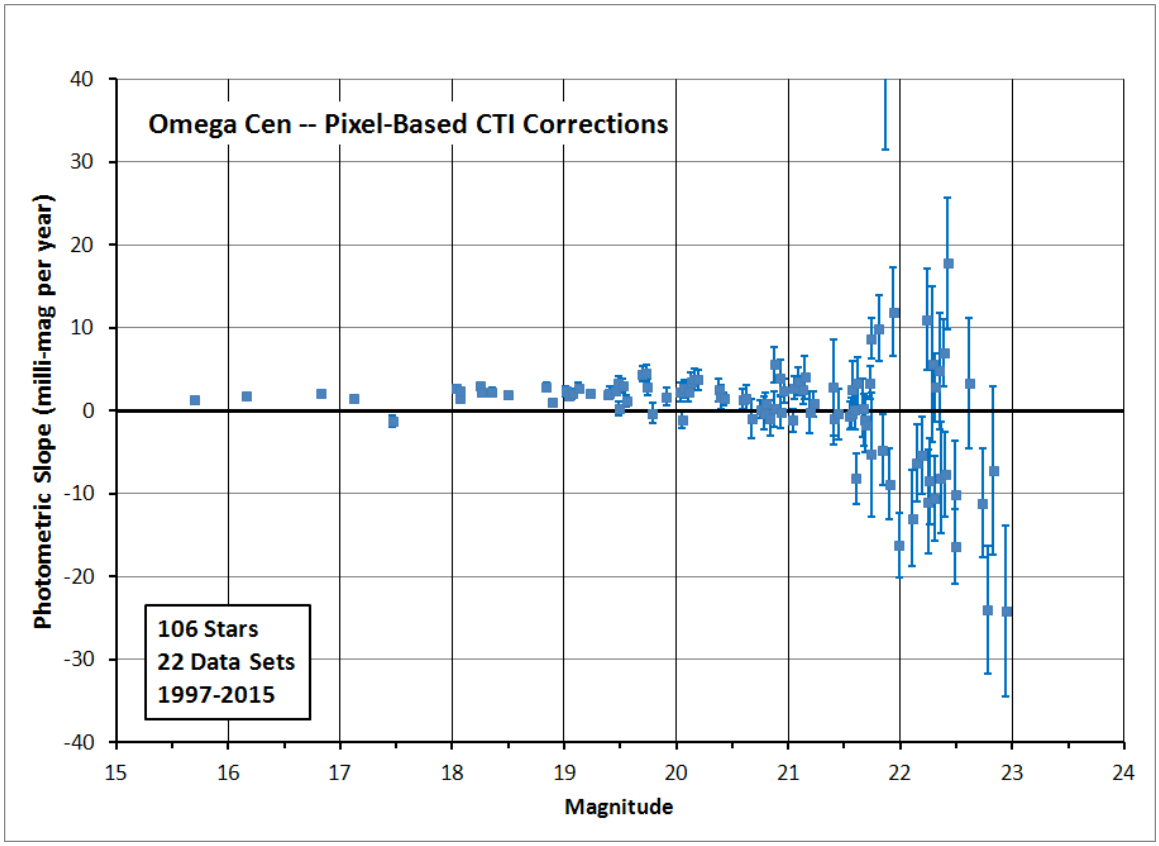

Figure 9. Long-term photometric slope plotted against magnitude for 106 stars with pixel-based CTI corrections applied.

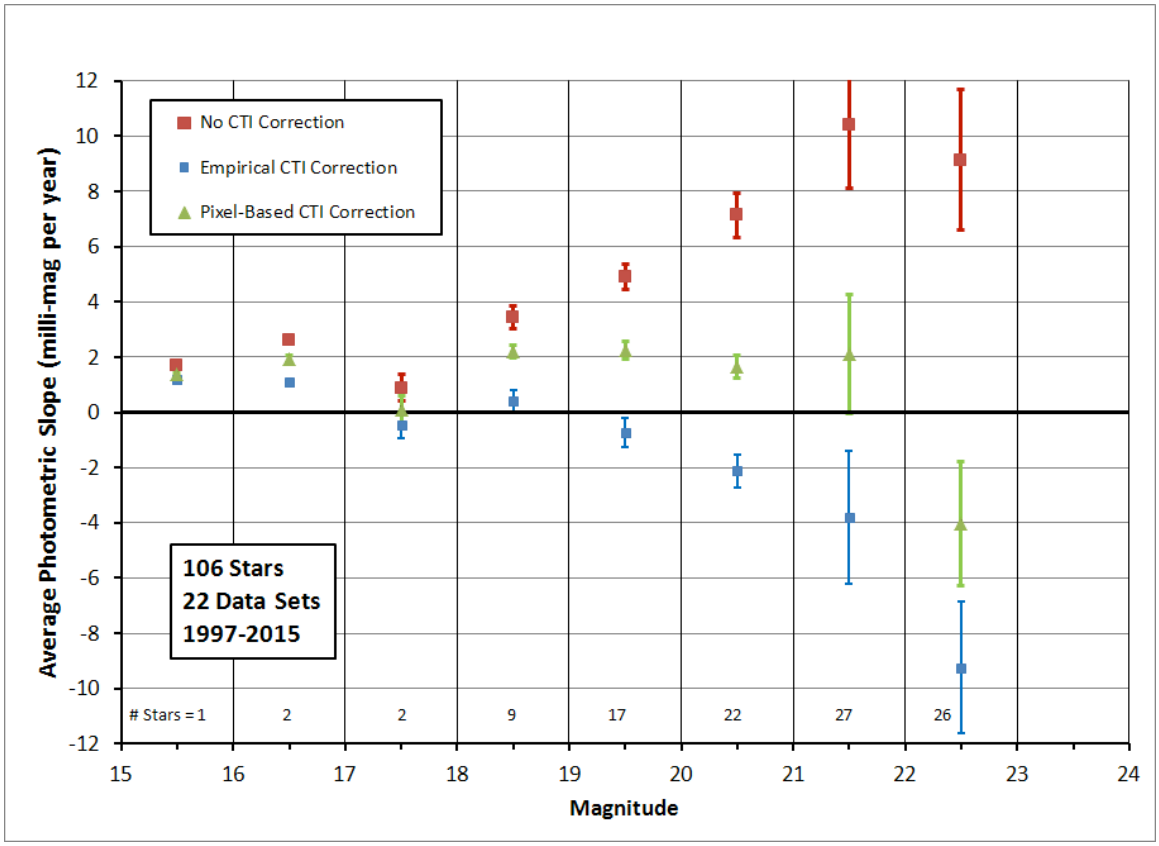

Figure 10. Long-term average photometric slope vs. magnitude. The data have been averaged in 1 magnitude bins, and the different CTI corrections are as labeled. The number of stars contributing to each bin is indicated near the bottom of the plot. The vertical scale is uncertain by about 1 to 2 milli-mag/yr due to TDS effects.

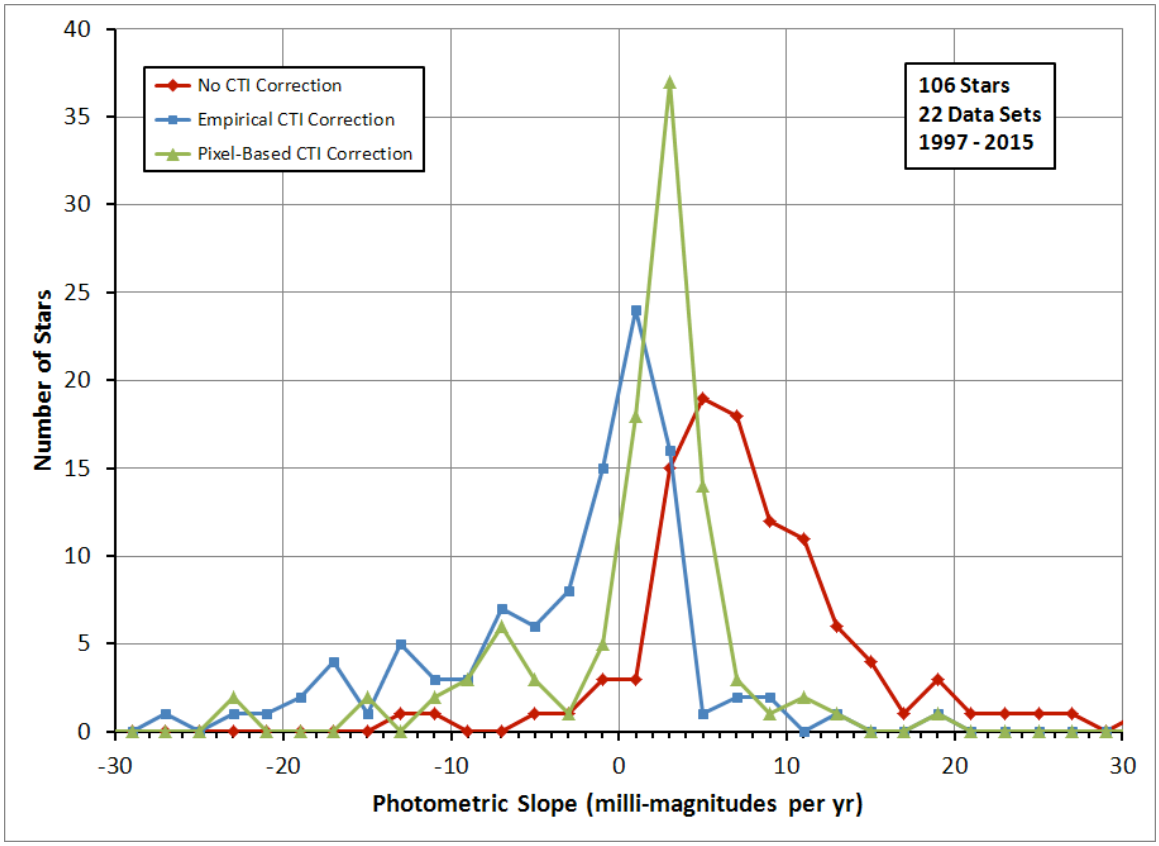

Figure 11. Histogram of photometric slopes for the three cases of CTI correction, empirical CTI corrections, and pixel-based CTI corrections. The bins are 0.002 milli-mag/yr wide.

3.2. Y-dependence of CTI Derived by Comparing Amps A vs. Amp D

The second test we apply to the CTI corrections is to compare stellar magnitudes for images read out with the CCD "A" amplifier against those for the identical target and pointing read out through the default CCD "D" amplifier. These amplifiers are at opposite ends of the CCD detector (Figure 12). Hence a star near the A amplifier will experience very little CTI when the image is read through the A amplifier, while the same star read out through the D amplifier will experience the maximum possible CTI. If the CTI corrections are working well, we should obtain the same magnitudes, regardless of which amplifier is used. Similar stellar photometry tests using opposite amplifiers have been previously performed for the ACS HRC (Chiaberge, et al., 2009) and the STIS CCD (Goudfrooij, et al., 2006).

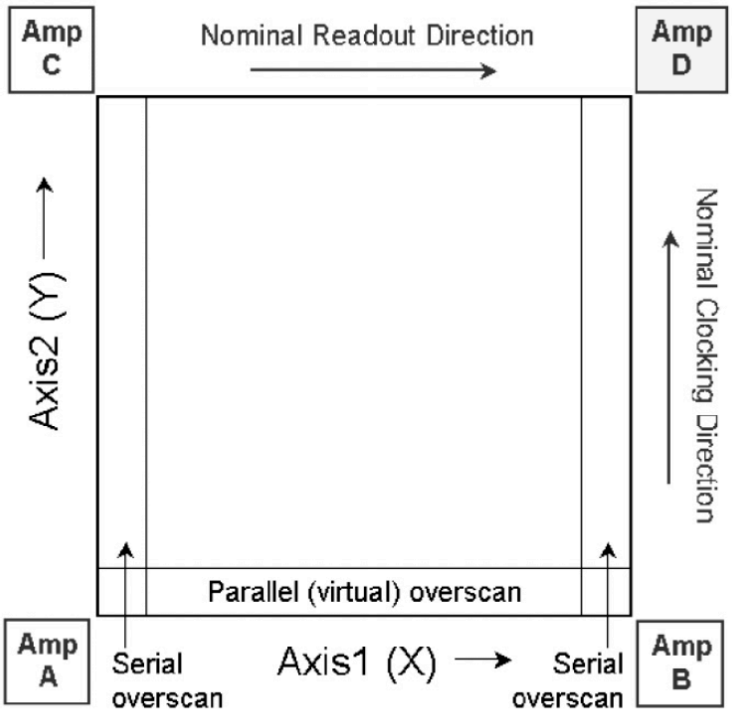

Figure 12. Locations of the A and D amplifiers. From Goudfrooij, et al., 2006.

As with the previous test, there are a number of advantages and disadvantages. The primary advantage is that it directly measures one of the fundamental properties of CTI – the detector Y-dependence. There are also no TDS dependence effects, since we can compare images taken during the same HST visit. And again we are comparing images of the same star with itself with the same exposure time, so there is no concern about photometric biases for bright vs. faint images, or calibration between different

instruments. There are also many Omega Cen images which have been taken in pairs between the A and D amplifiers.

The primary disadvantage of this method is that images taken with the A amplifier are not well-calibrated. The A amplifier gain has not been calibrated on-orbit. Bias and dark frames are infrequently taken in the A amplifier. And finally, the pixel-based CTI correction parameters have not been derived for the A amplifier. We will use work-arounds for these issues, but the situation is not ideal.

We selected the 2012 images obuo01050 and obuo01090 for this test (Table 1), since they are near the middle of the post-recovery era.[6] The "D" amplifier image utilzed the normal pipeline calibration reference files, but special reference files were created for the amplifier "A" image. A bias reference file was created from 18 amp A gain 4 bias frames taken between 12/1/2011 and 3/10/2012, which bracketed the Omega Cen data. Usually dark calibration is performed using dark files taken during the same week as the target observation, but no such dark frames were available. Instead, an amp A dark reference file was created from eight amp A gain 1 dark frames taken between 12/2/2011 and 12/19/2011 – these were the closest in time available.[7] The gain 1 dark file was scaled to gain 4 prior to being applied to the Omega Cen data. The calibrated amp A and amp D Omega Cen images used for this test are shown in Figure 13.

[6] Our first priority is CTI corrections for data taken after the STIS recovery in 2009.
[7] These dark frames were bias-calibrated using an amp A gain 1 bias reference file constructed from 15 bias frames taken between 11/1/2011 and 1/11/2012.

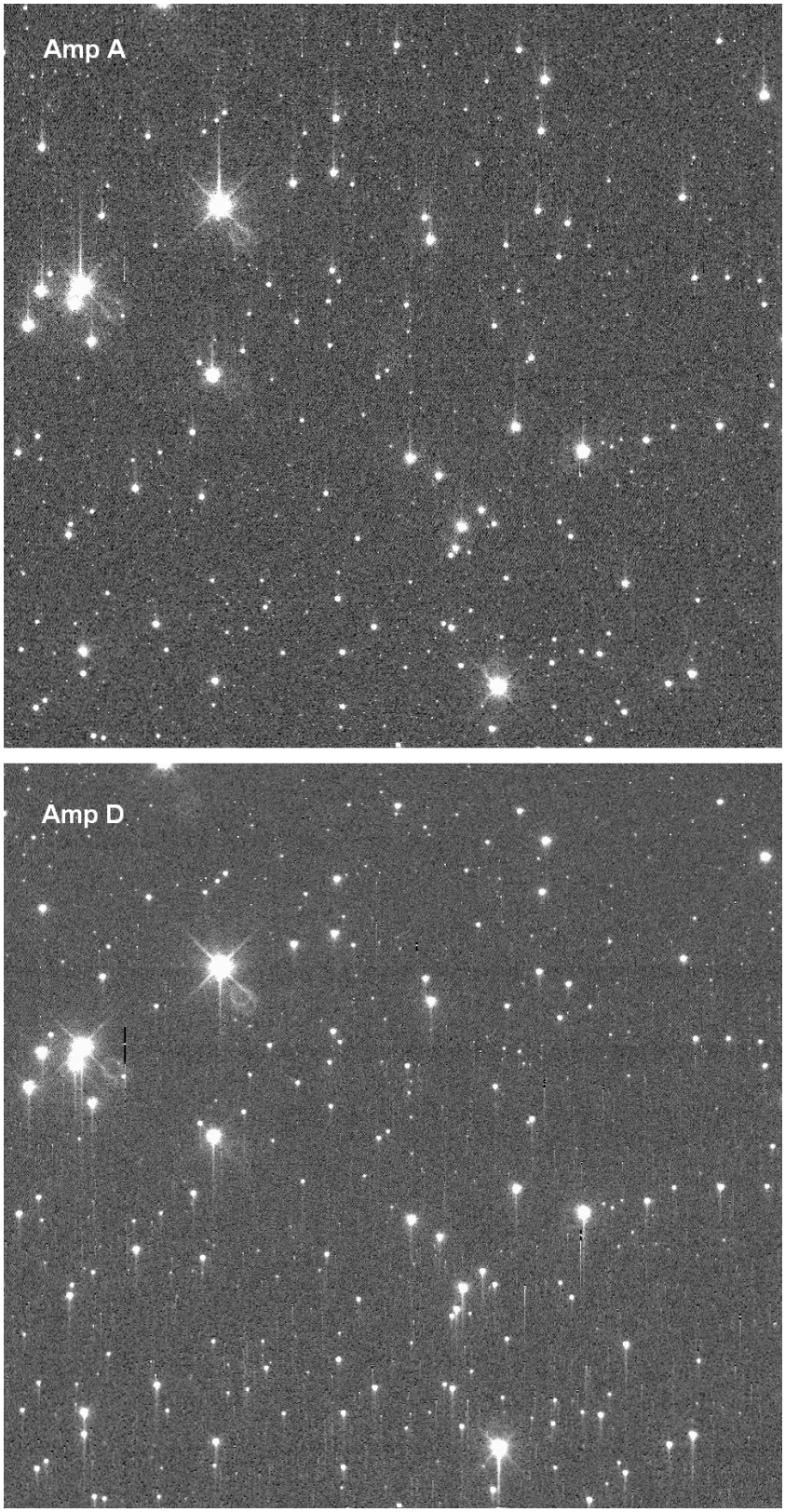

Figure 13. Calibrated amp A (obuo01090_sx2.fits) and amp D (obuo01050_sx2.fits) images. Note the CTI tails pointing in opposite directions in the amp A and amp D images.

Pixel-based CTI corrections on the amp A data were performed by assuming they had the same corrections as the amp D data. This is a reasonable assumption, since the CTI effects occur on surface of the CCD detector, and should be independent of the amplifier properties. Other properties, like the read-out speed, are identical between amps A and D. The amp A data were bias calibrated, the rows were flipped in the Y-direction (row [x,1] was moved to row [x,1024], etc.), the pixels were loaded into an amp D image fits file, and then the pixel-based CTI corrections were calculated in the usual way. After CTI correction the image rows were flipped back to the normal arragement, and the remaining calibrations (flat fielding, cosmic ray rejection, etc.) were applied.

Photometry was performed on the images as previously discussed. We divide the data into different magnitude ranges as the effects will depend on brightness (for this purpose we used the uncorrected magnitude averaged between the A and D amplifiers). The resulting photometry is presented in Figure 15 to Figure 19 in the Appendix. These plots show the difference between the magnitudes measured with the A and D amplifiers, i.e., [Mag(amp A) – Mag(amp D)], plotted against the Y position of the star on the detector. When no CTI corrections are applied, stars near the A amplifier (low Y vlaue) are brighter when read-out through the amp A than when read through amp D, and hence the magnitude difference [Mag(amp A) – Mag(amp D)] is negative. Conversely, stars near the D amplifier (high Y value) are brighter when read through amp D, and the magnitude difference is positive. Hence uncorrected data will tend to show a positive slope, as seen, e.g., in the top panel of Figure 15.

One might expect the magnitude difference at the center of the detector (Y=512) to be zero, but instead it is -0.05 in most of the plots. This is likely caused by a small difference in the gains of the A and D amplifiers. The gain of the A amplifier has not been measured on-orbit, so we cannot confirm this, but apparently it produces about 5% more counts per electron than the D amplifier.

The slope of the fitted line in these plots has native units of [Mag(amp A) – Mag(amp D)] per pixel. But we can multiply this by 1024 pixels (rows), divide by 2, and obtain a more intuitive quantity, which is the magnitude change across the 1024 rows of the detector for a single amplifier (e.g. amp D).[8] This resulting slope values are compiled in Table 3 and plotted for each magnitude bin in Figure 14.[9]

[8] The division by two is needed since we want the result for a single amplifier. For example, consider a case where the CTI across 1024 rows is 1 mag. A star at row Y=1 has, e.g., mag=10 and mag=11 for amps A and D, respectively. A star at row Y=1024 has, e.g., mag=11 and mag=10, for amps A and D, respectively. Hence we have data points Y and [Mag(ampA) – Mag(ampD)] of (Y=1, delta-mag= -1) and (Y=1024, delta-mag= +1). The slope of the fitted line would be 2 mag / 1024 pixels. Hence we need to divide by two to get the CTI effect for a single amplifier across 1024 pixels.

[9] This calculation makes the implicit assumption that CTI is identical for the two amplifiers, consistent with our prior assumptions.

When no CTI corrections are made, the magnitude change across the 1024 rows of the detector increases steadily from ~0.02 magnitude for the brightest stars, to ~0.27 magnitude for stars in the range 21-22 magnitude.

Both the empirical and pixel-based CTI corrections greatly reduce the magnitude change across the detector. The empirical CTI corrections tend to *over-correct* the CTI, and produce magnitudes which get brighter far from the amplifier. The resulting magnitude changes are -0.02 magnitude for bright stars, and steadily become more over-corrected, and reach -0.11 magnitude for stars in the 21-22 magnitude range. The pixel-based corrections tend to *under-correct* the CTI. Their correction is near perfect for bright stars, and steadily under-corrects, reaching about +0.08 magnitude for stars in the 21-22 magnitude range. These results are qualitatively similar to those found in the long-term photometry trend test discussed in section A and illustrated in Figure 10.

We can also express the over-correction or under-correction in terms of the size of the CTI effect. For the empirical corrections, the over-correction is small for the 18-19 magnitude bin, and is about 15% of the uncorrected CTI. For fainter stars in the 19-22 magnitude range, the over-correction is larger, and about 26% to 42% of the CTI effect. For the pixel-based corrections, the under-correction is about 40% in the 18-19 magnitude range, and is about 29% to 34% for stars in the 19-22 magnitude range. In this sense, the empirical and pixel-based corrections give similar performance for the fainter stars – their errors are similar in size.

We have omitted results for stars fainter than 22 magnitude, as the results are rapidly impacted by a combination of noise, high CTI losses, and artifiacts from poor calibration of the amp A data. The photometery software begins to have difficulty locating the stars far from the amplifier, as evidenced by large position discrepancies (many pixels) we saw between the A and D amplifier images. While nearly all stars in the 21-22 magnitude range had consistent positions between amp A and D images, about half the images had discrepant positions in the 22-23 magnitude range. This may be due to poor calibration of the amp A images, which leads to many residual hot pixels and other artifacts.

Table 3. Measured magnitude change across 1024 detector rows for a single amplifier.

	CTI Correction		
Magnitude Range	None	Empirical	Pixel-Based
15-18	+0.016 ± 0.004	–0.019 ± 0.004	+0.001 ± 0.004
18-19	+0.100 ± 0.007	–0.015 ± 0.008	+0.040 ± 0.008

19-20	+0.133 ± 0.011	–0.030 ± 0.010	+0.045 ± 0.010
20-21	+0.193 ± 0.015	–0.050 ± 0.015	+0.065 ± 0.015
21-22	+0.268 ± 0.033	–0.112 ± 0.033	+0.078 ± 0.032

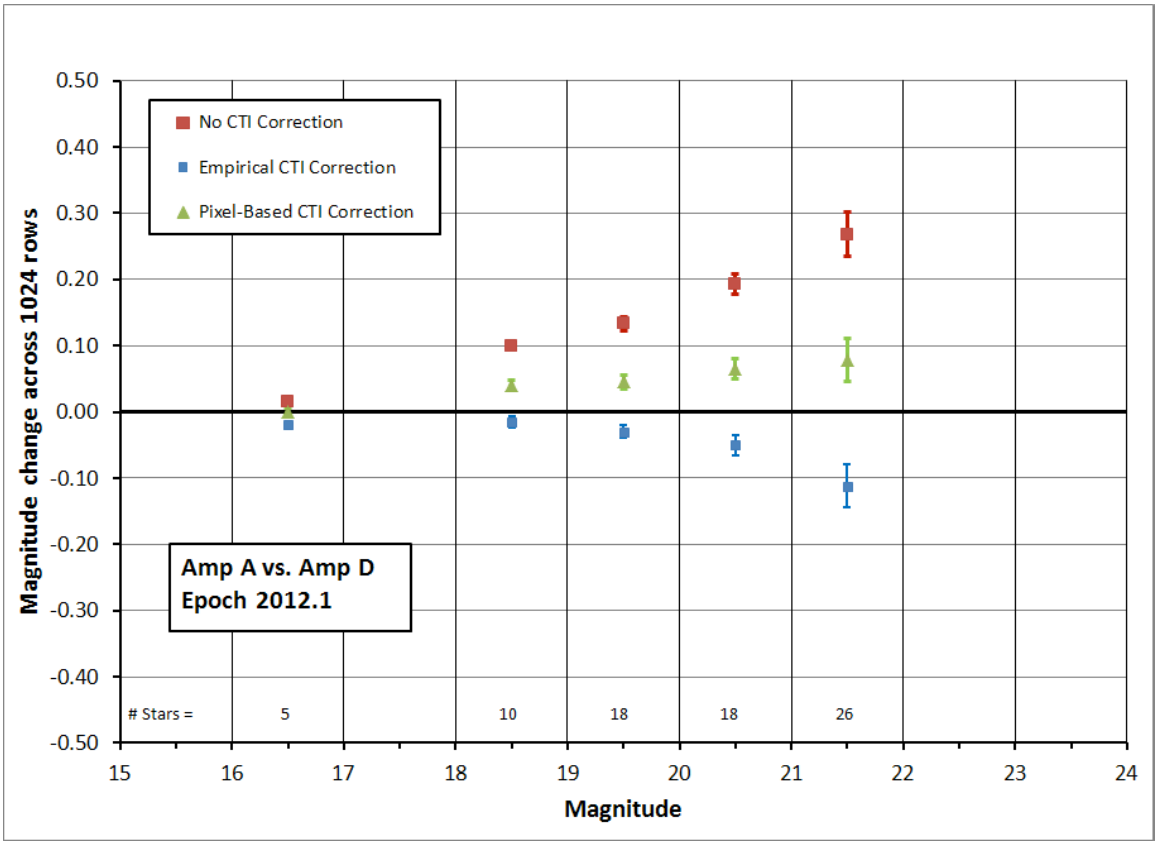

Figure 14. Measured magnitude change across 1024 rows plotted against magnitude. Results are given for five magnitude bins: 15-18, 18-19, 19-20, 20-21, and 21-22. The number of stars in each bin is given near the bottom of the plot. Data are from Table 3.

4. Summary

We have compared the empirical CTI corrections and the pixel-based CTI corrections for imaging photometry on Omega Cen using two different tests. The first test examines the long-term photometric trend using 22 datasets spanning the STIS mission, while the second test explicitly examines the Y-dependence of CTI by comparing amp A and amp D data at a single epoch in 2012. These two tests draw on relatively independent data sets, having only the 2012.1 amp D dataset in common.

The two tests give qualitatively and quantitatively similar results. Both tests indicate the

empirical CTI corrections and pixel-based CTI corrections significantly improve the photometry as compared to uncorrected data. We also find that the empirical corrections tend to *over*-correct the CTI, while the pixel-based corrections *under*-correct the CTI, as seen in both tests in Figure 10 and Figure 14. These errors, while different in sign between the two corrections, are similar in size.

The exact behaviors of the two corrections depend on stellar magnitude. For the brightest stars (mag= 15 to 18) the CTI effects themselves are very small. The amp A vs. amp D test shows the pixel-based corrections appear to give the best accuracy in this magnitude range, but the differences from no correction and empirical corrections are only ~0.01 magnitude at the CCD center (Table 3, Figure 14). For the long-term trend test, the results are similar, but the differences are also comparable in size to the uncertainties related to TDS effects (Figure 10).

Between 18 and 19 magnitude, the empirical corrections tend to give near-perfect correction in the amp A vs. amp D test, while the pixel-based corrections only correct about 50% of the CTI. However, the error here is relatively small for the pixel-based corrections in terms magnitudes. In Figure 14 – the stars are too faint by ~0.04 magnitude far from the amplifier, or ~0.02 magnitude near the center of the detector. For the long-term test the empirical corrections again appear to give perfect correction, but the differences between the empirical corrections and pixel-based corrections are similar in size to the uncertainties related to TDS effects.

For fainter stars in the range 19 to 22 magnitude, the empirical corrections *over*-correct the CTI by 26% to 42%, while the pixel-based corrections *under*-correct by about 29 to 34% of the total CTI effect (based on the amp A vs amp D test in Figure 14). Similar results are seen in the long-term photometry test in Figure 10. In this magnitude range the CTI effects are large, and both the empirical and pixel-based corrections are significantly better than no correction.

At the faintest magnitudes (mag=22 to 23) the pixel-based corrections appear superior to the empirical corrections (Figure 10), but the uncertainties on the data are large.

The pixel-based corrections appear to give somewhat better stability than the empirical corrections across different magnitude regimes. This is evident as a tighter histogram in Figure 11, a flatter distribution in Figure 9, and smaller range of values in Table 3. Hence the pixel-based corrections might be preferable when good relative photometry is needed.

5. Future

There are many other tests which would be interesting to perform, but have been omitted here for lack of data or analysis time. It would be interesting to pursue CTI measurements where Omega Cen was observed with the well-calibrated amp D with the star cluster rotated 180 degrees on the detector. This type of test has generally been used with good success on other instruments. There are some STIS CCD data available in 2001 and 2002 with the detector rotated 180 degrees on the sky – for example data sets o6ib01020_sx2.fits and o6ib02020_sx2.fits. But these data are early in the mission when CTI was small. It would be very interesting to take new data of a similar nature late in the mission. This would require a new single orbit on Omega Cen in August or September 2015 or 2016. This would allow the entire test to be performed with the well-calibrated amp D. The impact of TDS effects would be minimal since the time span between observations would be only 6 months.

There are also more epochs of amplifier A data already in hand that could be processed, compared against the amplifier D data, and checked for results similar to those above. This might give added confidence to the results in section B above, though of course the same issues with the amp A calibrations would exist. It might be possible to take additional amp A Omega Cen data in the future where bias and dark calibration images in amp A are also obtained at the same time. This might even be implemented by merely re-scheduling existing amp A calibrations to coincide better in time with the amp A Omega Cen observations. This would greatly improve rejection of hot pixels that impact the photometry for the fainter stars.

Many of these same proposals also contain short (e.g. 2 second) exposures that could be used to measure CTI at lower stellar counts and lower sky background levels. It might also be possible to compare the long and short duration exposures, and directly study the brightness dependence of CTI effects, though great care would be needed so as to avoid biases in the photometric procedures (i.e. systematic errors in estimating and subtracting the sky counts, etc.). Perhaps better photometry software would be needed to do this successfully.

There are also more faint stars availble in the images presented here, but their uncertainties would be large, and it is not clear whether there are enough numbers of faint stars so as to average-out the increased scatter.

We thank Julia Roman-Duval for providing her IDL photometry code, and for her patience while answering many questions related to the code. We also thank Charles Proffitt and Jay Anderson for many helpful discussions.

References

Anderson, J., and Bedin, L. R., 2010, "An Empirical Pixel-Based Correction for Imperfect CTE. I. *HST* 's Advanced Camera for Surveys," PASP, 122, 1035.

Bohlin, R. C., and Goudfrooij, P., 2003, "An Algorithm for Correcting CTE Loss in Spectrophotometry of Point Sources with the STIS CCD," Instrument Science Report STIS 2003-03R.

Chiaberge, M., Lim, P.-L., Kozhurina-Platais, V., and Sirianni, M., 2009, "Updated CTE photometric correction for WFC and HRC," Instrument Science Report ACS 2009-01.

Gilliland, R., Goudfrooij, P., and Kimble, R. A., 1999, "Linearity and High Signal-to-Noise Performance of the STIS CCD," PASP 111, 1009.

Goudfrooij, P., Bohlin, R. C., Maiz-Apellaniz, J., and Kimble, R. A., 2006, "Empirical Corrections for Charge Transfer Inefficiency and Associated Centroid Shifts for STIS CCD Observations," PASP 118, 1455.

Lockwood, S., 2012, "STIS CTE Parameter Fitting," https://confluence.stsci.edu/download/attachments/50631094/Lockwood%20--%20CTI_parameter_model_whitepaper.pdf?api=v2, internal report.

Lockwood, S., et al., 2013, "Towards a Pixel-Based CTE Correction of the STIS CCD," https://confluence.stsci.edu/download/attachments/50631094/Lockwood%20--%20AAS%20Poster%202013-01.pdf?api=v2, AAS Meeting #221.

Lockwood, S., et al., 2014a, "Progress Towards a STIS Pixel-Based CTI-Correction," HST Calibration Workshop, https://confluence.stsci.edu/download/attachments/50631094/Lockwood%20--%20Cal%20Workshop%202014-08.pdf?api=v2.

Lockwood, S., 2014b, "Fine-Tuning the CTI Correction Parameters," https://confluence.stsci.edu/download/attachments/50637560/cti_fine_tuning_v2.pdf?version=1&modificationDate=1422316072000&api=v2, internal report.

Lockwood, S., et al. 2015, "Pixel-Based CTI Corrections for the STIS CCD," Instrument Science Report STIS 2015-xx, in preparation.

Roman-Duval, J., and Proffitt, C., 2013, "Full-field sensitivity and its time-dependence for the STIS CCD and MAMAs," Instrument Science Report STIS 2013-02 (RP2013).

Stys, D. J., Bohlin, R. C., and Goudfrooij, P., 2004, "Time-Dependent Sensitivity of the CCD and MAMA First- Order Modes," Instrument Science Report STIS 2004-04.

Appendix: Plots of [Mag(amp A) – Mag(amp D)] vs. Y

Below we give plots showing the photometric results obtained by differencing observations obtained with amp A from those obtained with amp D. All data are from epoch 2012.1. Image obuo01090_sx2.fits and obuo01050_sx2.fits are used for amp A and D, respectively. The plots are organized by star magnitude range (i.e. 15-18, 18-19, etc.). Each plot shows results for no CTI correction (top panel), empirical CTI correction (middle panel), and pixel-based CTI correction (bottom panel).

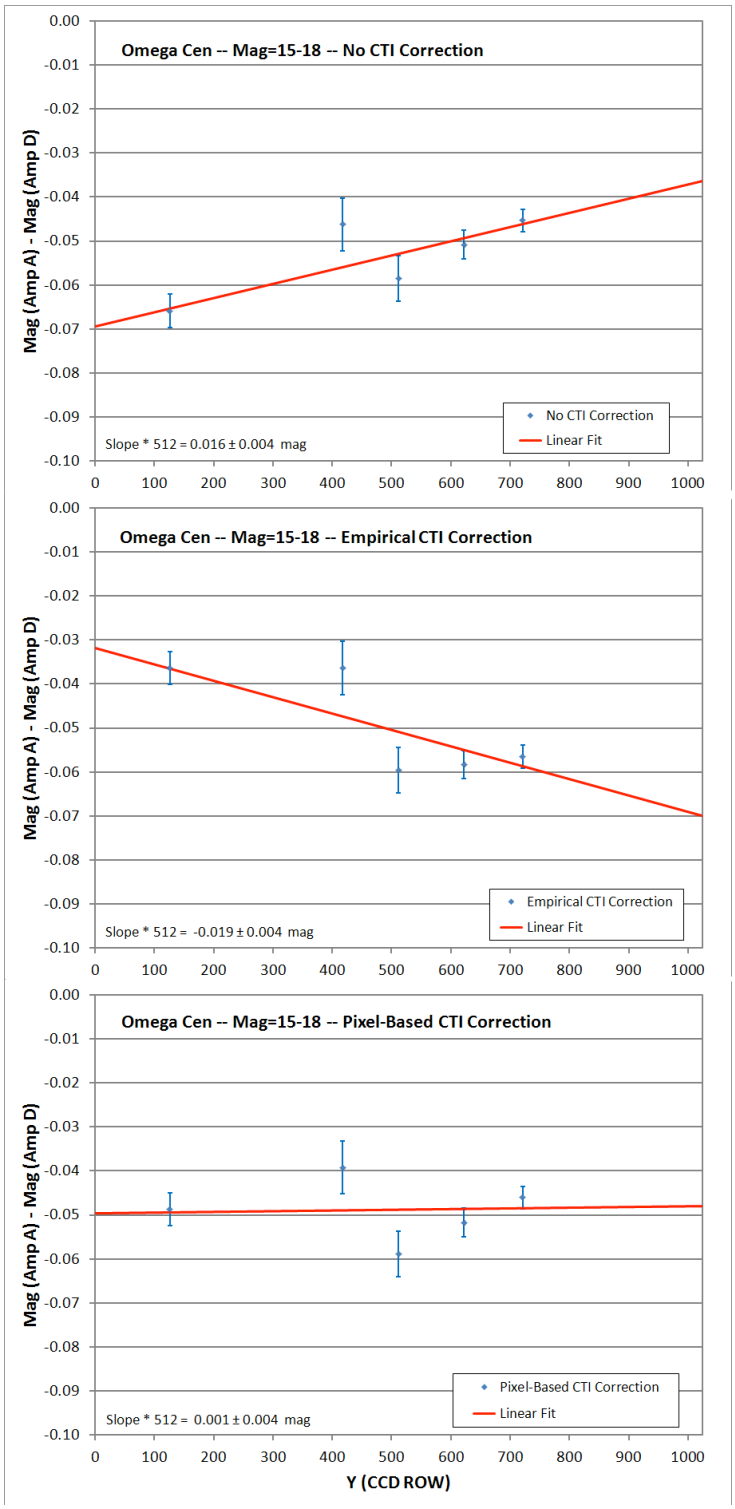

Figure 15. Plot of [mag (amp A) - mag (amp D)] vs. CCD row for magnitude 15 to 18 stars. The fitted lines have slopes as follows (magnitude change across 1024 detector rows for a single amplifier): Top panel: no CTI correction, slope +0.016 ± 0.004. Middle panel: empirical CTI correction, slope -0.019 ± 0.004. Bottom panel: pixel-based CTI correction, slope +0.001 ± 0.004.

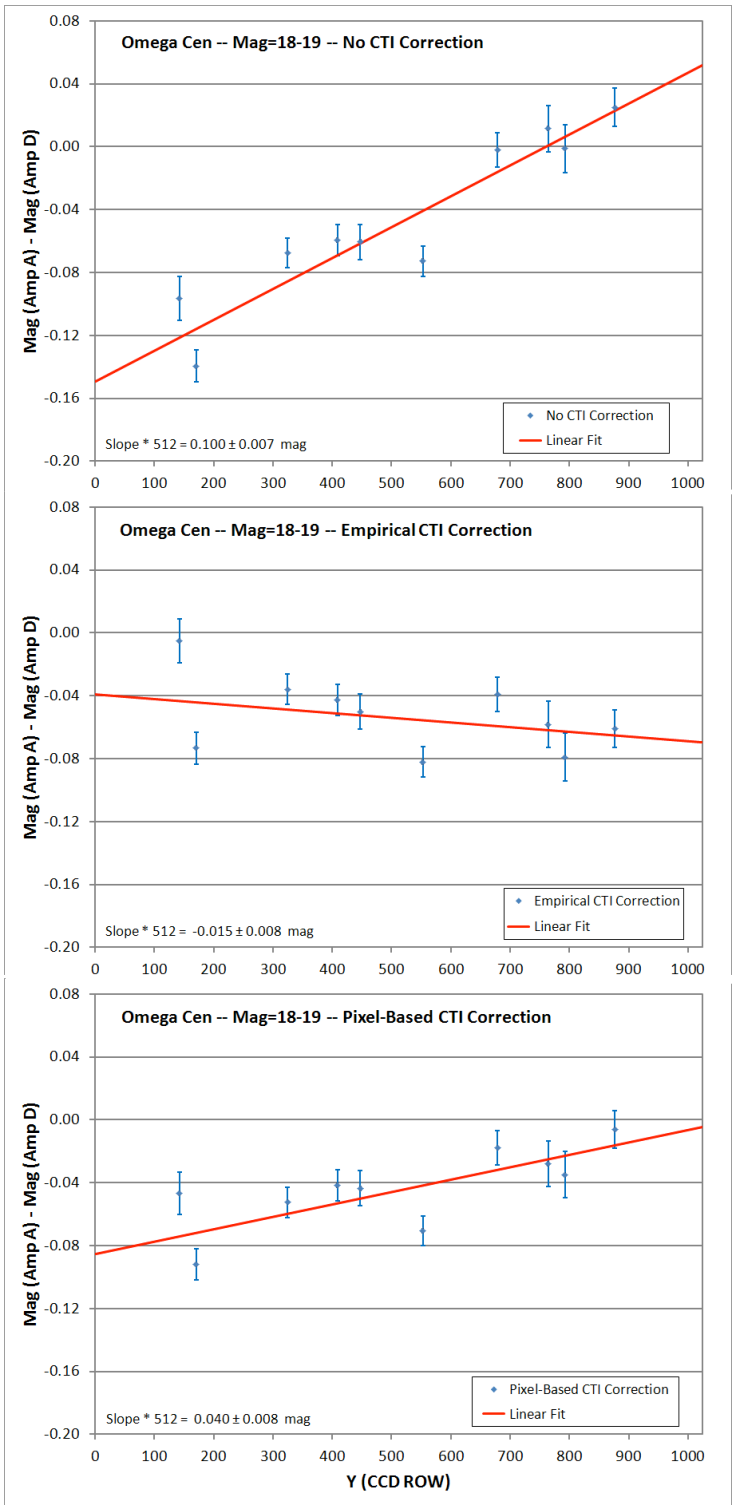

Figure 16. Plot of [mag (amp A) - mag (amp D)] vs. CCD row for magnitude 18 to 19 stars. The fitted lines have slopes as follows (magnitude change across 1024 detector rows for a single amplifier): Top panel: no CTI correction, slope +0.100 ± 0.007. Middle panel: empirical CTI correction, slope -0.015 ± 0.008. Bottom panel: pixel-based CTI correction, slope +0.040 ± 0.008.

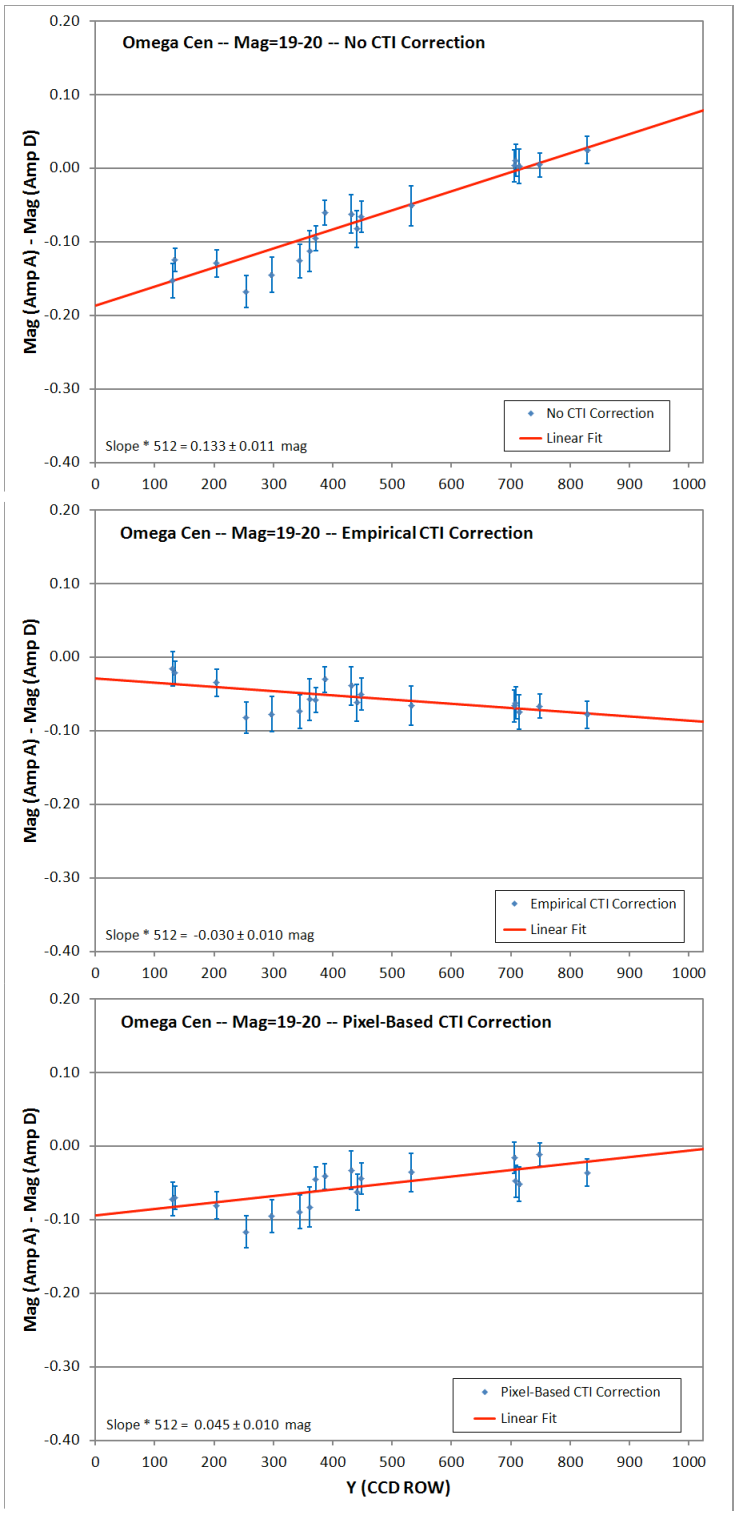

Figure 17. Plot of [mag (amp A) - mag (amp D)] vs. CCD row for magnitude 19 to 20. The fitted lines have slopes as follows (magnitude change across 1024 detector rows for a single amplifier): Top panel: no CTI correction, slope +0.133 ± 0.011. Middle panel: empirical CTI correction, slope -0.030 ± 0.010. Bottom panel: pixel-based CTI correction, slope +0.045 ± 0.010.

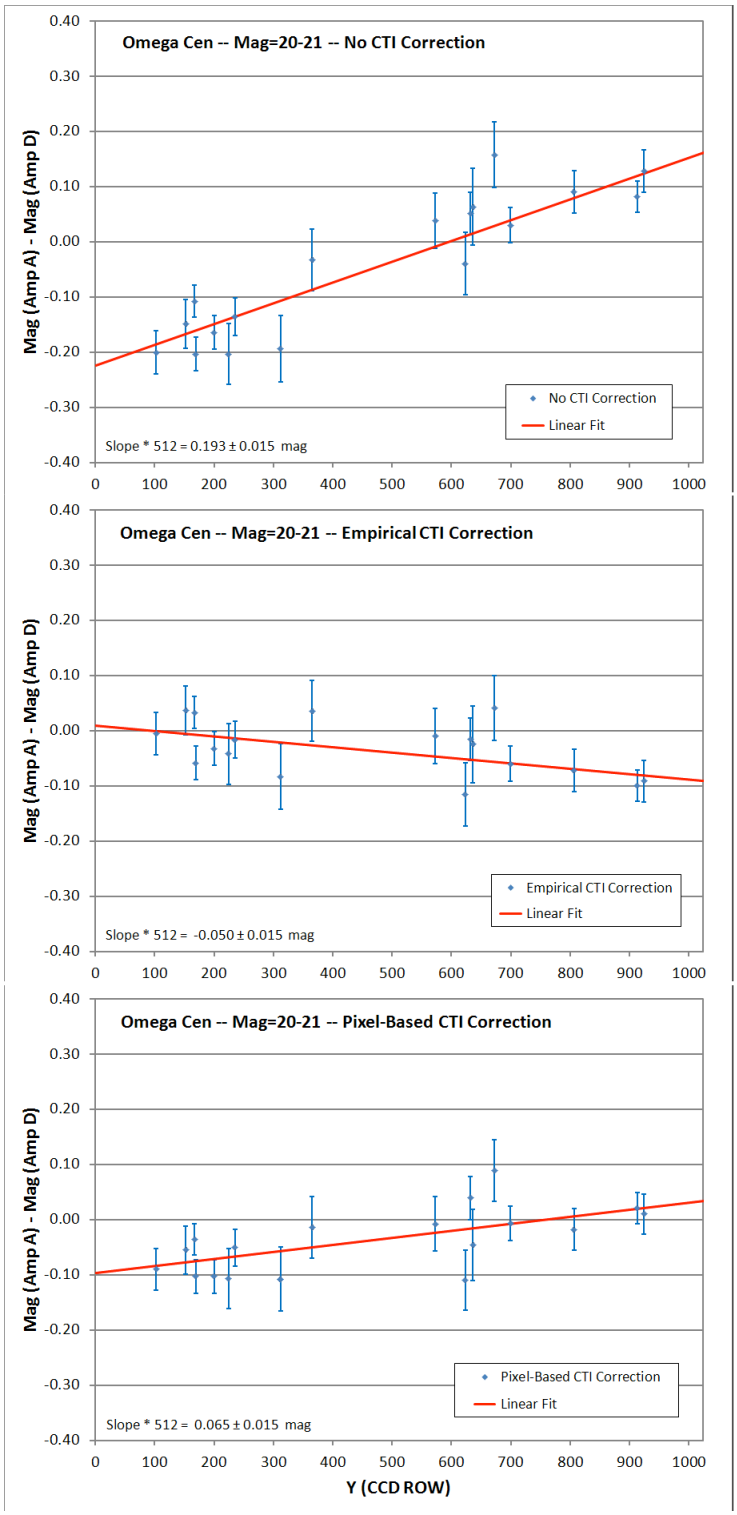

Figure 18. Plot of [mag (amp A) - mag (amp D)] vs. CCD row for magnitude 20 to 21. The fitted lines have slopes as follows (magnitude change across 1024 detector rows for a single amplifier): Top panel: no CTI correction, slope +0.193 ± 0.015. Middle panel: empirical CTI correction, slope -0.050 ± 0.015. Bottom panel: pixel-based CTI correction, slope +0.065 ± 0.015.

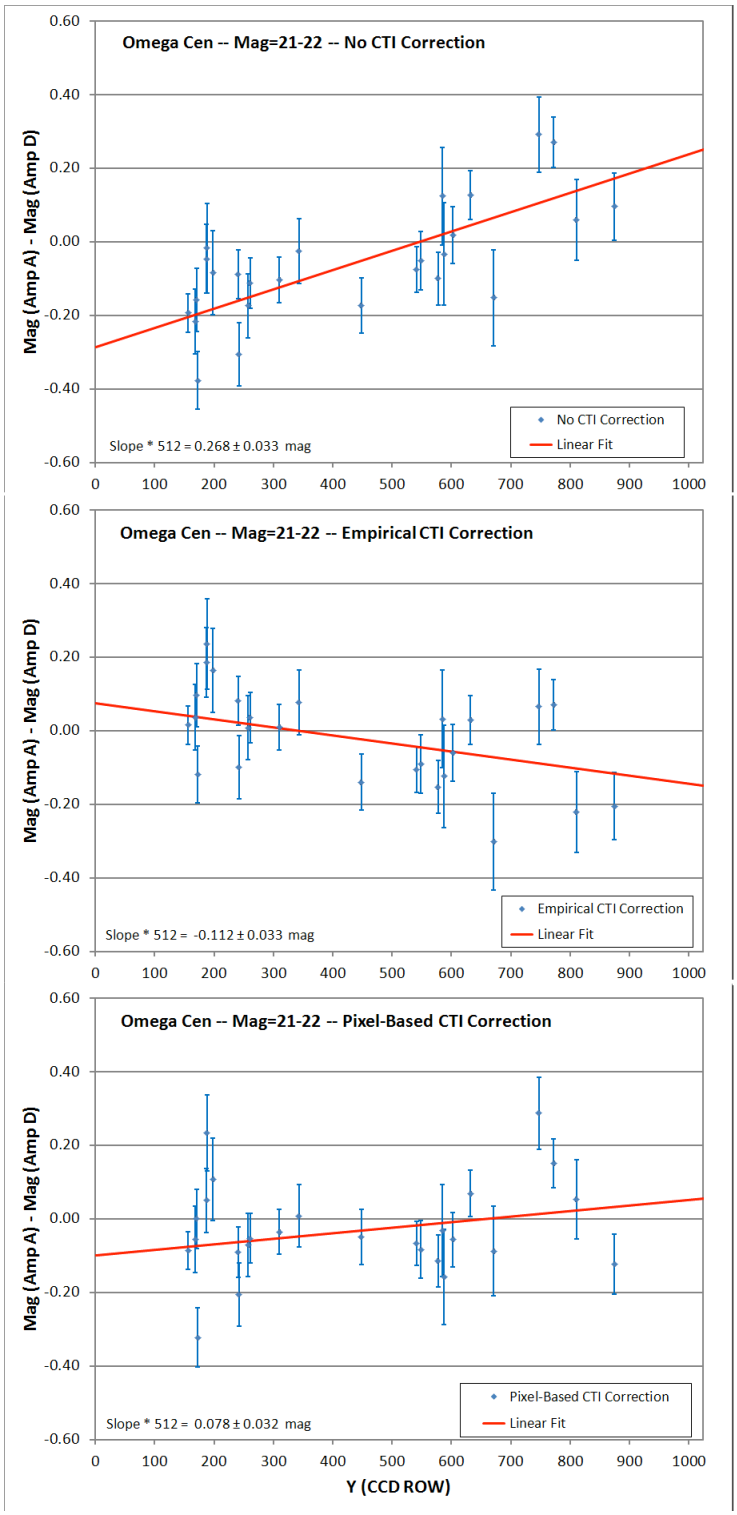

Figure 19. Plot of [mag (amp A) - mag (amp D)] vs. CCD row for magnitude 21 to 22 stars. The fitted lines have slopes as follows (magnitude change across 1024 detector rows for a single amplifier): Top panel: no CTI correction, slope +0.268 ± 0.033. Middle panel: empirical CTI correction, slope -0.112 ± 0.033. Bottom panel: pixel-based CTI correction, slope +0.078 ± 0.032.